Int. J. Nonlinear Anal. Appl. 15 (2024) 6, 263–278
ISSN: 2008-6822 (electronic)
http://dx.doi.org/10.22075/ijnaa.2023.30997.4537

Study of unreinforced masonry elements strengthened with engineered cementitious composites under impact loading

Seyedmohammad Amini[a], Alireza Mirjalili[b,*], Mohammadreza Javaheri[a]

[a]Department of Civil Engineering, Taft Branch, Islamic Azad University, Taft, Iran
[b]Department of Civil Engineering, Yazd Branch, Islamic Azad University, Yazd, Iran

(Communicated by Zakieh Avazzadeh)

Abstract

Given the brittle behavior and low flexibility of unreinforced masonry walls, using flexible fiber-reinforced concretes, such as engineered cementitious composites (ECCs), to retrofit them is of great importance. In this regard, the performance of these materials (as a reinforcement layer of unreinforced masonry walls) in improving their behavior (flexibility and strength) against dynamic loads, especially impact loads, should be taken into account. The present study evaluates and compares the vertical middle displacement, energy, and distribution of plastic strains in unreinforced masonry materials, under two conditions, i.e., non-retrofitted and retrofitted with a one-side cover (in the lower surface of the specimen) or two-side cover of ECC layers under dynamic impact loading, through nonlinear dynamic impact analysis. The ECC reinforcement layers in two-side covers were investigated by changing their location (in the middle or edges of the lower surfaces of the specimen), connection type (disconnection or full connection) of the one-side cover of the bottom of the specimen with the ECC reinforcement layer and elastic modulus (from 15 GPa to 22.5 GPa). The retrofitting of the unreinforced masonry materials with ECC layers (especially with two-side cover) improved their behavior against out-plane impact loads, dissipated energy, and reduced the plastic strains and cracks.

Keywords: Unreinforced masonry wall, engineered cementitious composite (ECC), reinforcement layer, out of plane impact load, finite element method, Abaqus software
2020 MSC: 74S05

1 Introduction

All over the world, many URM (unreinforced masonry) buildings are popular construction method preferred [20, 27]. Also, unreinforced masonry structures are of the largest share of decaying building stock around the world, and in many scenarios, they comprise high cultural value monuments left behind by history [21, 22]. Given their poor quality of construction and materials and lack of a sustainable design, the above buildings can barely withstand seismic movements [20].

To overcome this problem, URM structures may be reinforced by (confining) concrete elements with horizontal and vertical reinforcements so that CM (confined masonry) structures are formed, which are of efficient confinement for

*Corresponding author
Email addresses: s_m_amini66@yahoo.com (Seyedmohammad Amini), alireza.mirjalili@iau.ac.ir (Alireza Mirjalili), javaheri@taftiau.ac.ir (Mohammadreza Javaheri)

Received: March 2023 *Accepted:* June 2023

masonry walls and enhance the structures deformability [29, 34]. However, in case of excessively large spacing between the vertical elements (i.e. tie columns) or when the material used to fabricate the masonry panel confined by the tie elements is a mortar of low-strength, unreinforced masonry walls may bear serious damages [3, 5]. Also, in case of rare devastating seismic events, unreinforced confined masonry structures can be vulnerable to damages. Thus, especially in case of older buildings, one should apply reinforcing techniques to improve the CM structures behavior [5]. Among the advantages of unreinforced masonry buildings, one can refer to easy access to their constituent materials and their easy construction approaches. However, it is noteworthy that their construction techniques are very vulnerable to out-of-plane loadings such as heavy forces applied by wind and seismic activities. Given the above considerations, both techniques of post- and pre-retroftting strengthening for the structures exposed to acute seismic conditions are of the same significance [6, 8].

Unreinforced masonry walls present multiple modes of in-plane failures [18], and the failure type observed in walls depends on the characteristics of their constituent materials, the intensity of the axial loading that the wall is exposed to, and the geometry of the wall [13].

In recent years, the necessity of developing blast and impact-resistant retrofits and designs for buildings has led to a motivation for finding an effective technique to enhance the out-of-plane strength of unreinforced masonry walls. The primary actual defenses of the above structures against the effect of blast and impact loadings are the structure exteriors, which are of a masonry nature in general [16].

Among the most advanced kinds of high-performance fiber reinforced cementitious composites with properties including higher tensile-strain capacities as well as reliable strain-hardening performance, one can refer to ECCs (engineered cementitious composites) [33]. Engineered cementitious composites have been employed to retrofit the damaged and undamaged bearing unreinforced masonry walls. Conventional unreinforced cementitious materials do not present adequate strength capacity (typically < 3.5 MPa) and tensile strain (typically $< 0.015\%$ strain). Engineered cementitious composites are innovative composite materials featuring pseudo-strain hardening when in tension. Engineered cementitious composites have a matrix of Portland cement mortar or paste as well as a low volume fraction of fibers including PVA (polyvinyl alcohol) or UHMWPE (ultrahigh molecular weight polyethylene) fibers. According to the test results, the structural ductility, the shear resistance, and, the lateral stiffness are significantly enhanced for the retrofitted structural elements [5]. The fibers found in engineered cementitious composites improve the tensile strengths of the material from 2 to 8 MPa and its tensile strain capacity by 0.5 to 6% [10, 20]. Also, Iosipescu shear [35] and Ohno shear [12] tests may reveal the multiple cracking of the same material under shearing. Also, the numerical models presented by some authors for the masonry elements retrofitted through engineered cementitious composites have been validated and presented insights into the improved behavior of those structural elements retrofitted using the same material. Some studies have been conducted to determine the effect of this type of material on the behavior of masonry infilled and concrete structures. In particular, the retrofit configuration using full coating ECC could prevent the premature development of diagonal cracks, thereby preserving the integrity of the masonry walls at a large lateral displacement [23]. In general, engineered cementitious composites play a key role in enhancing the retrofitted structures behavior [5, 19].

In order to reproduce the nonlinear performance of the engineered cementitious composites as strengthening layers for out-of-plane performance improvement in the masonry, a multi-linear plastic material model was used by S. Pourfalah et al. [25, 26] in which the tri-linear stress–strain curve represents the tensile performance.

The effect of engineered cementitious composites mortar on the performance of the brick unreinforced masonry walls was the topic studied by Lin et al. [13]. According to their research results, engineered cementitious composites are effective in enhancement of both the pseudo-ductility and the inplane strength of unreinforced masonry walls. Also, it has been demonstrated that increased masonry wall thickness leads to decreased bonding between engineered cementitious composite layer and masonry wall. Given the fact that according to this research results, the ductility and strength of wall are greatly improved, the results should be scrutinized for a bearing unreinforced masonry wall with failure modes that differ from those of the Walls. For bearing unreinforced masonry walls, the in-plane failure modes include rocking behavior, bed-joint sliding, toe crushing, and diagonal tension cracking. Some parameters e.g. the gravity load level, the materials properties, and the wall dimensions can affect the above modes of failure [20]. A study was conducted by Deng and Yang [4] on the behavior of unreinforced masonry walls retrofitted with engineered cementitious composites mortar. They constructed six half-scale specimens that included retrofitted and un-retrofitted walls, which were tested via static cyclic lateral loading. Of the above walls, two of them were retrofitted using engineered cementitious composite mortar with strip pattern, whilst the other two were entirely retrofitted by applying a constant thickness of engineered cementitious composite mortar. Their research results showed that the above retrofitting approaches may effectively enhance the displacement ductility and lateral strength in unreinforced masonry walls. In addition, in accordance with the test results, different patterns implemented for engineered cementitious

composite mortar may lead to varied modes of failure in retrofitted walls. The rocking and diagonal failure modes took place for the fully coated and strip patterns, respectively, whilst the diagonal failure mode occured for that of the un-retrofitted walls. Generally, according to the results of this research, some parameters including the loading conditions, wall properties, implemented patterns of ECC mortar and the retrofitting details can significantly affect the lateral strength, energy absorption, and failure mode of the retrofitted unreinforced masonry wall [20].

Zhang et al. [36] developed a hybrid-fiber engineered cementitious composite by employing an appropriate volume ratio of low and high modulus fibers, so that the functional requirements for blast- and impact-resistant structures are met in a better manner. The hybrid-fiber engineered cementitious composite mix contained 1.5% PE (polyethylene) and 0.5% steel fibers (by volume), and showed an optimum equilibrium between strain capacity and ultimate strength. An experimental study was conducted by Maalej et al. [17] to examine the resistance of high velocity impact of the same hybrid-fiber engineered cementitious composite that approved its capability to withstand multiple impacts with little spalling, small crater size and fragment ejection on the impact face and its high capacity of energy absorbance. In addition to the mechanical characteristics of engineered cementitious composite cited so far, later studies by Li and Li [11] have also certified engineered cementitious composite as a noticeable material used for repairs. The study approved that the for the repair material, its ductility is vital to ensure its durability within the renovated structure. Especially, when exposed to drying shrinkage circumstances, the engineered cementitious composite is of a high tensile ductility relaxing the likely stress build-ups in the repair layers. The same behavior realized through several micro-crack damages minimizing the interfacial delamination. Singh et al. [30] also investigated the out-of-plane performance of a URM sandwich-like ECC-based beam coupled with epoxy material. It was discovered that using prefabricated ECC boosts the stiffness and deformability of masonry beams [32]. Thus, one can consider ECC as a suitable material employed to strengthen URM structures exposed to blast/impact loading [16].

This study is mainly aimed at making an experimental investigation on the effectiveness and performance of masonry walls strengthened by ECC to withstand out-of-plane impact and quasi-static loadings. Load-bearing walls are among the main structural components of masonry buildings as they resist gravitational and lateral loads. The poor performance and failure of such components can lead to localized and progressive failure in the building, destabilization, and collapse. As the most critical structural components, load-bearing walls must be evaluated and retrofitted, particularly for dynamic loads (e.g., impact loads). The use of specific concrete lining enables the in-plane and out-of-plane behavior improvement of such walls. Engineered cementitious composites (ECCs) and their effects on the behavior of brick walls have not been studied in Iran. The novelty of the present study arises from the specific characteristics of mortars and bricks in Iran.

2 Materials and method

2.1 Methodology

The finite element method (FEM) is typically utilized to simulate structural components and analyze their dynamic behavior. As the most commonly used method in continuous settings, FEM has been widely employed in the micro- and macro-modeling and dynamic analysis of complex engineering problems, such as structural components, in recent decades. FEM utilizes explicit (time-dependent) or implicit formulations.

ABAQUS is among the most powerful FEM software packs that can employ both explicit and implicit formulations. It uses two- and three-dimensional elements in continuous settings and can perform the micro- and macro-simulation of structural components (e.g., masonry walls) and fiber-reinforced concretes (e.g., ECCs). Thus, FEM allows for modeling ECC-retrofitted URM walls and analyze the dynamic impact behavior of such models. As a result, the present study adopted ABAQUS micro-scale three-dimensional simulations where:

- Homogenous mass based on the elastoplastic behavior model (using a hybrid plastic-failure model to define plastic masonry behavior) to model the equivalent blocks of the masonry units and the surrounding mortar,
- Contact elements with a proper behavior model are employed to simulate the connection of the equivalent blocks,
- Homogenous mass based on the elastoplastic behavior model (using a hybrid plastic-failure model to define the plastic behavior of ECC) to model ECC layers,
- Proper boundary conditions are applied to the specimens to stabilize the numerical models, and
- The nonlinear dynamic analysis of the specimens is performed under impact loading while evaluating the out-of-plane behavior (i.e., ductility and strength) of the specimens under the load.

2.2 Numerical simulations validation

In this study, the results of micro and three-dimensional numerical simulations during a loading test on a wall sample with unreinforced unretrofitted materials are compared to the measured data from the experiments in order to validate the method of numerical simulations and the software employed for this purpose (Abaqus software).

2.2.1 Numerical simulation of the laboratory sample

The lateral load-bearing of the sample during nonlinear static analysis under uniform lateral loading is assessed and corresponded with this load measured from the investigation to validate the method of numerical simulations and the software employed for this objective (Abaqus software) with micro and three-dimensional numerical simulation during a uniform loading examination on a wall sample containing unreinforced unretrofitted building materials (brick type) in a study conducted by Papanicolaou et al. [22].

The explicit analytical process is employed in the micro and three-dimensional numerical simulation of this investigation. The steps of this simulation are described in the following section. The explanation of these steps also includes additional test characteristics.

2.2.2 Laboratory sample modeling

It should be noted that the bricks' length and height, as well as the thickness of the mortar in the horizontal and vertical gaps between them, are taken into consideration to disregard the numerical simulation of the mortar (in micro and 3D numerical simulation). Therefore, the experimental sample necessitates numerical modeling of the interaction between the adjacent equivalent bricks in order to describe the mortar behavior in the horizontal and vertical gaps between the bricks. On the interface of adjacent equivalent bricks, contact elements with shear and normal behavior are employed for this objective. Therefore, it is essential to take into account adhesion and friction coefficient (roughness level) in these interfaces in order to characterize the shear behavior of these elements.

A linear elastic behavior model are employed to numerically model the upper and lower concrete beams in the experimental sample (Fig. 1). The tie is employed to numerically simulate the communication of the upper and lower concrete beams with the top and bottom of the wall under the supposition of complete restraint at these beams and the wall interface. The following definition will be used in the sequel.

2.2.3 Boundary settings modeling of the laboratory sample

All translational and rotational deflections in the floor of the experimental sample (lower surface of the lower concrete beam) are tied to stabilize the numerical model (Fig. 1). [21, 22].

2.2.4 Laboratory sample loading

Following the application of a uniform vertical surcharge of 390 kPa to the upper concrete beam's upper surface, the lateral surface of the upper concrete beam is subjected to a predefined uniform lateral deflection step by step (3.5 mm) in order to numerically load the experimental sample and determine the lateral load-bearing of the sample during loading. The sample is afterward analyzed using a nonlinear static method with uniform lateral loading (Fig. 1).

2.2.5 Model meshing

Eight-node continuous three-dimensional elements with attenuated integration (referred to as C3D8R in Abaqus [15]) are employed for meshing masses in the numerical model.

2.3 Assessment and validation of the study's numerical simulation findings for the laboratory sample

Now, the lateral load-bearing capacity of the laboratory sample during the analysis is assessed by the nonlinear static method under uniform lateral loading to guarantee the precision of numerical simulations and the software employed for this objective (Abaqus software) in the research. Afterward, according to Table 1, it corresponds with the load-bearing measured during the experiment.

When the predefined uniform lateral deflection is applied to the laboratory sample step by step during the nonlinear static analysis of the sample, excellent agreement (with a maximum tolerance of about 6.3%) between the lateral load-bearing calculated during the experiment and the load-bearing measured from the experiment is shown Table 1. This demonstrates confidence in the accuracy of the numerical simulations and the software employed in the investigation (Abaqus).

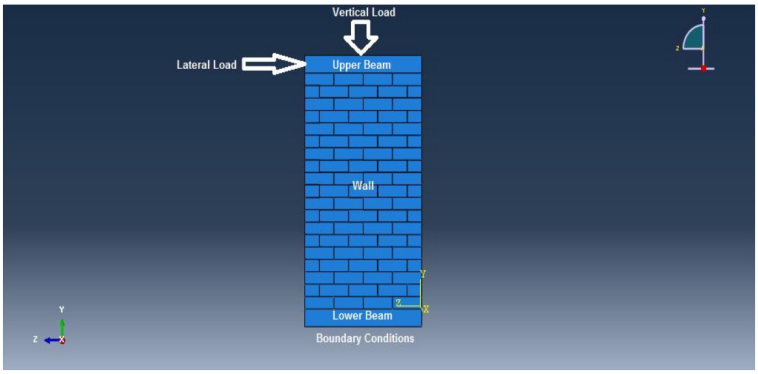

Figure 1: Geometric model for the laboratory sample

Table 1: The maximum lateral load-bearing of the laboratory sample during the experiment [22] and numerical analysis

Max. Lateral Bearing (KN) (Experimental)	**Max. Lateral Bearing (KN) (Numerical)**	**Tolerance (%)**
6.35	6.75	6.3

2.4 Experimental works using experimental specimens

To investigate the behavior of ECC-retrofitted unreinforced masonry (URM) buildings under impact loads, it is required to evaluate the ECC thickness, the number of ECC layers, and the ECC type. Thus, a minimum of two factors should be considered for each parameter. A minimum of three specimens should be fabricated for each factor. In addition, the combined effects of these parameters are to be studied. A total of 18 specimens were fabricated. Six specimens were built to study the effects of the ECC layer location (i.e., top and/or top and bottom layers). Six specimens were employed to study the ECC layer position (completely contentious or a discontinuity in the middle of the specimen). Also, three specimens were employed as the control specimens, while the remaining three specimens were used to explore the combined effects of the parameters.

Once the experimental specimens had been fabricated based on the required parameters, the impact test was applied to the specimens. The impact process was recorded by specific cameras, analyzing the impact loads of the specimens using the software. Then, the micro-scale and three-dimensional simulations of both ECC-retrofitted and non-retrofitted URM specimens were carried out based on the given geometric and mechanical parameters. The boundary conditions and meshing were applied to the specimens. Then, the subjects were subjected to impact loads. The nonlinear dynamic analysis of the specimens under the impact loads was carried out to evaluate the out-of-plane behavior (ductility and strength) of the specimens under the loads.

2.5 Non-reinforced masonry modeling

For micro numerical modeling of bricks in the non-reinforced masonry sample, 10 isotropic and homogeneous masses are used as follows:

1. As equivalent blocks (containing masonry unit and its adjacent mortar).
2. With a layout according to figures 5 and 6 to 14 [26].
3. With a length, width, and height of 210, 75, and 102 mm, respectively [26].
4. With an elastoplastic behavior by employing a plastic-damage combination model for defining the plastic behavior

The simplified micro approach has been used to model non-reinforced masonry in 3D simulations. As part of this method, masonry is modeled by equivalent blocks containing masonry units and their mortar proximity. A brick (65 mm wide [26]) and half of its adjacent mortar (10 mm thick [2]) are considered equivalent blocks (75 mm wide), which will be connected by suitable contacts. So, the numerical modeling of the interaction between adjacent bricks is required for defining the behavior due to the mortar (available in joints between bricks) in the non-reinforced masonry sample. Hence, contact elements (with shear and normal behavior) are used at the interface of adjacent bricks, where the friction coefficient (surface roughness) is critical for determining the shear behavior of the elements.

Notably, the specific weight, elasticity modulus, Poisson's ratio, compressive strength, tensile strength, and dilation of equivalent models are 18.5 KN/m^3, 3500 Mpa, 60 Mpa, 6 Mpa, and 10 degrees, respectively [26]. In addition to

defining the physical and elastic properties of equivalent models, the plastic behavior and properties will also be defined. Therefore, a combined plastic-damage model was used for bricks, which is a continuous plastic model for considering the damage standard of the brick (using two principal failure mechanisms of the brick i.e., tensile cracking, and compressive crushing) according to the following properties [7, 14]:

1. Brick's strain-stress curve under uniaxial compressive force
2. Brick's strain-stress curve under uniaxial tensile force

For defining the strain-stress curve of the brick under uniaxial force, a connection between compressive strain and stress of the brick is required. For this purpose, the following equation is used in the simulation [9]:

$$\sigma_c = f'_c[2(\varepsilon_c/\varepsilon'_c) - (\varepsilon_c/\varepsilon'_c)^2] \tag{2.1}$$

Where σ_c and ε_c are compressive strain and stress, respectively, f'_c and ε'_c are brick's compressive strength (in this simulation 60 Mpa) and its corresponding strain (0.0024 in this simulation according to Park and Paulay [24]), respectively.

This equation creates a curve in which the brick's behavior is linear after reaching the compressive strength of the brick. It continues after reaching 20% of this strength because the brick keeps 20% of its compressive strength in high compressive strains [14]. Therefore, according to the curve and the equation, compressive plastic strains are calculated for compressive strength and used for defining the compressive plastic behavior of the equivalent blocks. In the following, the strain-stress curve of the brick under uniaxial tension is defined regarding the brick tensile strength (6 Mpa in this simulation) and linear elastic behavior for the brick until reaching the tensile strength (strain-stress curve peak under uniaxial tension).

2.6 Modeling of ECC layers in the non-reinforced masonry sample

For numerical modeling of ECC layers in the non-reinforced masonry sample, homogenous masses are used:

1. With the considered thickness (t)
2. On the sample's bottom or top surfaces, either in whole or in part
3. With or without a total connection with the bottom or top surfaces of the sample
4. Elastoplastic behavior model using a plastic-damage combined model for defining the plastic behavior.

The tie constraint is used to numerically model a complete connection for ECC layers to the non-reinforced masonry sample, assuming that the sample and layers interfaces are fixed. Also, numerical modeling of the incomplete connection between ECC layers and the non-reinforced masonry sample is defined using contact elements (with normal and shear behavior) at these interfaces. It is crucial to consider the coefficient factor (surface roughness) when defining the shear behavior of these elements. In addition to defining the physical and elastic properties of ECC layers, the plastic behavior and properties will also be defined. For this purpose, a combined plastic-damage model is used for ECC layers. As mentioned, the model is a continuous plastic model for considering the damage criteria of materials (using two principal failure mechanisms i.e., tensile cracking and compressive crushing) [7, 14].

So, first, the compressive strain-stress curve of ECC layers is defined according to Table 2 (obtained from the compressive test on the ECC) [28]. In the following, tensile stress-strain curve values of ECC layers will be defined according to Table 3 (obtained from the tensile test on ECC).

Table 2: Values of the stress-strain of stress curve of ECC layers [28]

Yield Stress (MPa)	**Inelastic Strain** $\times 10^{-3}$
19.62	0.00
28.08	2.80
36.79	5.70
49.60	9.90
56.89	12.70
62.78	17.00

2.7 Boundary conditions modeling

For numerical models stability, transitional displacements on two sides of models are restrained (in latitudinal direction) (Figures 7 to 14) [26].

Table 3: Values of the stress-strain of tension curve of ECC layers [28]

Yield Stress (MPa)	**Inelastic Strain** $\times 10^{-3}$
1.45	0.00
1.06	5.70
0.43	13.80

2.7.1 Impact loading

Usually, the effect time of this type of loads (td) is relatively short. If it is very small compared to the time of free vibration of the device, then it can be assumed that the maximum response of the device is achieved in a very short time interval, before the damping forces have the opportunity to absorb energy. For this reason, the damping effect is ignored in the dynamic analysis of devices against such forces [1].

When a beam with a unit width is subjected to an impact load, it finds an instantaneous transverse velocity V_0 in such a way that it satisfies the principle of linear motion.

Result;

$$(2ml)V_0 = (P_0 2L)\tau \tag{2.2}$$

$$V_0 = \frac{P_0 \tau}{m} \tag{2.3}$$

in this case;

$$T = mV_0/P_c \tag{2.4}$$

$$w_f = mV_0^2 L^2/3M_0 \tag{2.5}$$

where T is the response time and W is the maximum permanent transverse displacement, m is the mass, P_0 is the initial load and $P_c = 2M_0/L^2$ is the static collapse pressure of the beam and M is the bending moment [31].

2.7.2 Impact loading of the models

Models are examined and compared using an impact vertical load (under a time-load curve in Fig. 2 [30]) applied to the middles, and the vertical displacement, energy, intensity, and distribution process of plastic strains of the models are investigated (figures 2 to 3).

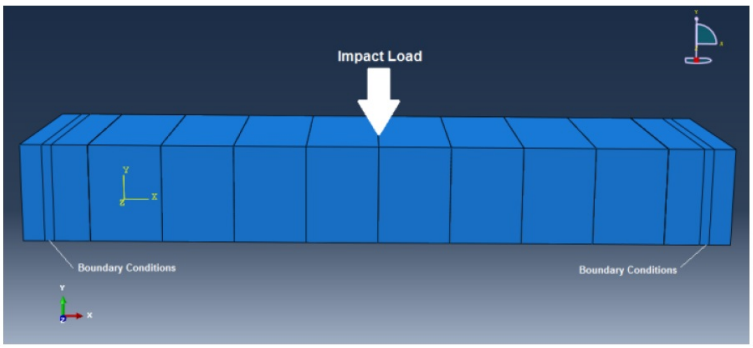

Figure 2: Geometric model of the non-reinforced non-retrofitted masonry sample

2.7.3 Models meshing

Continuous 3D 8 node elements (known as C3D8 in the Abaqus software [15]) are used for meshing masses in models.

3 Results and Discussion

In the present section, vertical displacement, energy as well as the plastic strains intensity and procedure of non-reinforced masonry material sample under two various conditions including retrofitting and non- retrofitting with

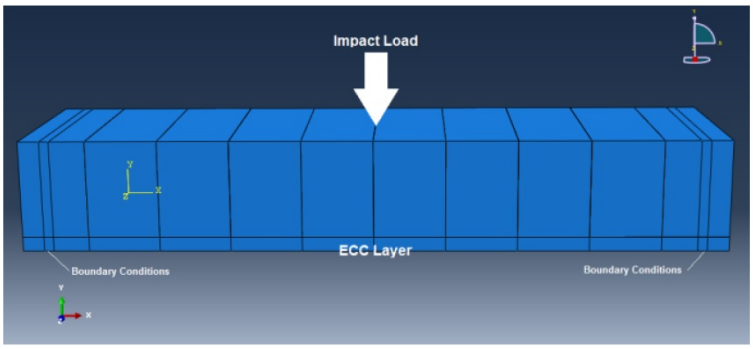

Figure 3: Geometric model of the non-reinforced retrofitted masonry sample with one layer of ECC in the whole of the sample bottom surface

one-sided coating (with two positions- on the above and below surface of the sample) and double-sided coating of ECC layers during vertical impact loading (during non-linear dynamic analysis) of the middle of the sample are investigated. In addition, the effect of ECC reinforcement layers on the out-of-plane dynamic loading behavior of unreinforced building material walls, the role of double-sided coating (compared to one-sided coating) and the position of ECC reinforced layers (on the top or bottom of the sample) are also studied.

In the meantime, changing the location of ECC reinforced layers -where is assumed in the middle or on the above and bottom surfaces of the sample- in the two-sided coating, changing the connection in one sided coating of the bottom surface of the sample with ECC reinforced layer, changing the thickness (from 7.5 to 30 mm) and modulus of elasticity (from 15 to 22.5 GPa) of ECC reinforced layers in two-sided coating, the role of location (in the middle or on the sides of the above and bottom surfaces of the sample) reinforced with ECC layers, type of connection (detachment or complete connection) of ECC reinforced layers with building materials as well as the hardness and thickness of ECC reinforcement layers in the extent of this effect ECC reinforcement layers are studied on the impact dynamic behavior of off-plane walls of unreinforced building materials.

3.1 Assessment of the results obtained from numerical simulations in the research

It is worth noting that according to the figures of the dimensionless parameters, the reduction percentages of the vertical displacement in the middle ($\Delta U/U_0$), energy ($\Delta E/E_0$), and plastic strain ($\Delta\varepsilon/\varepsilon_0$) of the specimen were also evaluated in each mode. In these parameters, U_0, E_0, and ε_0 are the maximum vertical displacement in the middle, energy, and plastic strain of the non-retrofitted unreinforced masonry materials, respectively. Accordingly, $\Delta U, \Delta E$, and ΔE denote the difference between the values of the corresponding parameters, respectively, under two conditions, i.e., non-retrofitted and retrofitted with ECC layers.

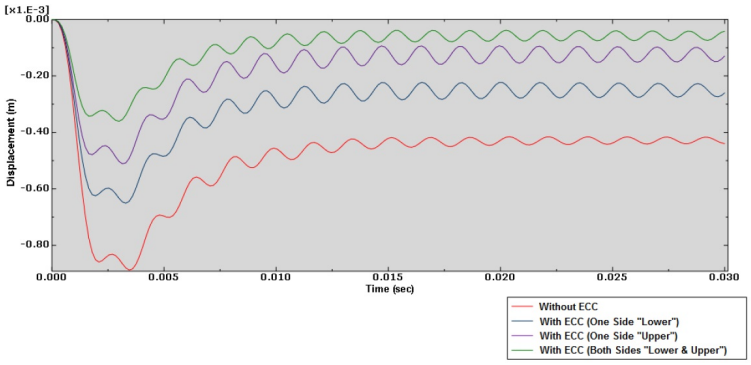

Figure 4: The effect of the ECC reinforcement layers and the location of these layers (with full connection) on the vertical displacement in the middle of the unreinforced masonry material specimen during vertical impact loading (t = 15 mm, E_{ecc}=17.5 GPa)

According to Figs. 4 and 5, the retrofitting of the unreinforced masonry material specimen with ECC layers (especially with a two-side cover) significantly increases the stiffness and, eventually, the out-plane strength of the specimen under impact loading, resulting in a remarkable reduction in the vertical impact displacement in the middle of the specimen. It can also be seen that retrofitting the unreinforced masonry material specimen with the one-sided

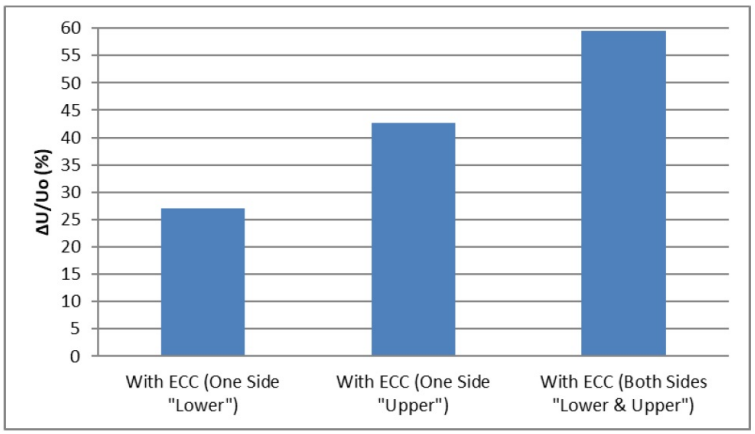

Figure 5: The effect of the ECC reinforcement layers and the location of these layers (with full connection) on the percentage of reduction in the vertical displacement in the middle of the unreinforced masonry material specimen during vertical impact loading (t = 15 mm, E_{ecc}=17.5 GPa)

cover of the ECC layer on the upper surface have a more significant performance in increasing the out-plane strength and finally reducing the vertical displacement in the middle of the specimen under impact loading.

Therefore, the figures above indicate the proper performance of the ECC reinforcement layers in reducing the deflections of the unreinforced masonry material specimen under impact loading and finally improving its out-plane dynamic impact behavior. With the two-sided cover of the specimen with ECC reinforcement layers (compared to the one-sided cover, especially on the lower surface of the specimen), this proper performance is more significant.

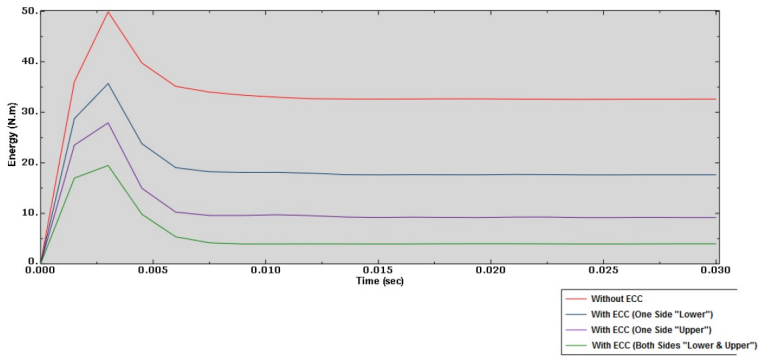

Figure 6: The effect of the ECC reinforcement layers and the location of these layers (with full connection) on the energy of the unreinforced masonry material specimen during vertical impact loading (t = 15 mm, E_{ecc}=17.5 GPa)

According to Figs. 6 and 7, the retrofitting of the unreinforced masonry material specimen with ECC layers (especially with a two-side cover) results in the energy absorption of the specimen under impact loading, which led to the more remarkable energy dissipation. It can also be seen that retrofitting the unreinforced masonry material specimen with the one-sided cover of the ECC layer on the upper surface had a more significant performance in energy absorption and, finally, energy dissipation under impact loading. Accordingly, the figures above indicate the proper performance of the ECC reinforcement layers in energy dissipation of the unreinforced masonry material specimen under impact loading and finally improving its out-plane dynamic impact behavior. With the two-sided cover of the specimen with ECC reinforcement layers (compared to the one-sided cover, especially on the lower surface of the specimen), this proper performance is more reliable.

Figs. 8 and 9 describe that retrofitting the unreinforced masonry material specimen with ECC layers (especially with a two-sided cover) remarkably lowers the concentration of the plastic strains in the edges of the specimen (and consequently cracking and failure of the specimen) under impact loading. The distribution of the concentrated strains and cracks (in the edges of the specimen) with a uniform trend through the specimen (especially in ECC layers) significantly reduces the intensity of plastic strains and the cracks and failure of the unreinforced masonry material specimen reinforced with ECC layers (especially with a two-sided cover) during the impact loading. It can also be said that retrofitting the unreinforced masonry material specimen with the one-sided cover of the ECC layer on the upper

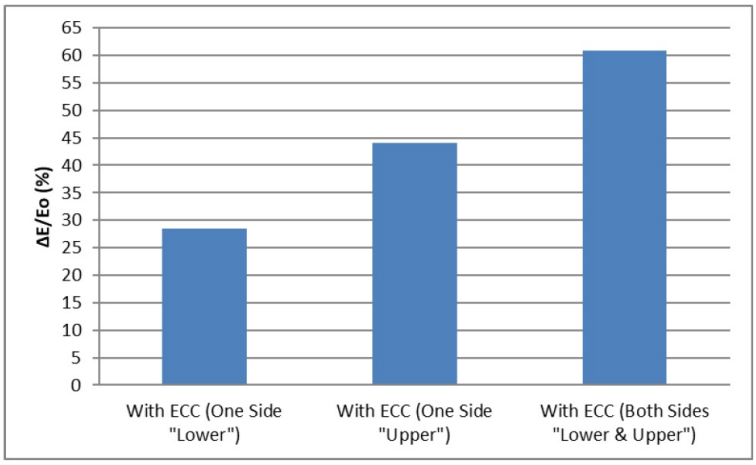

Figure 7: The effect of the ECC reinforcement layers and the location of these layers (with full connection) on the percentage of reduction in the energy of the unreinforced masonry material specimen during vertical impact loading (t = 15 mm, E_{ecc}=17.5 GPa)

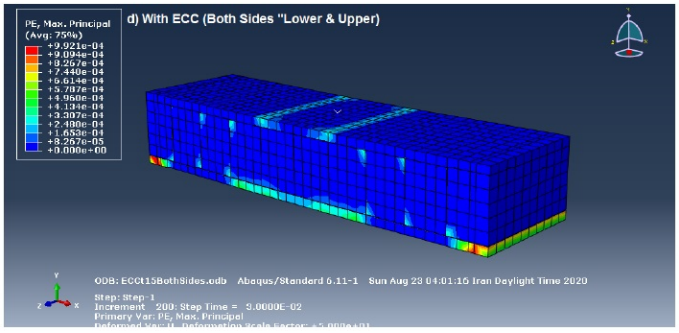

Figure 8: The effect of the ECC reinforcement layers and the location of these layers (with full connection) on the strain intensity and distribution of the specimen of unreinforced masonry materials during vertical impact loading (t = 15 mm, E_{ecc}=17.5 GPa)

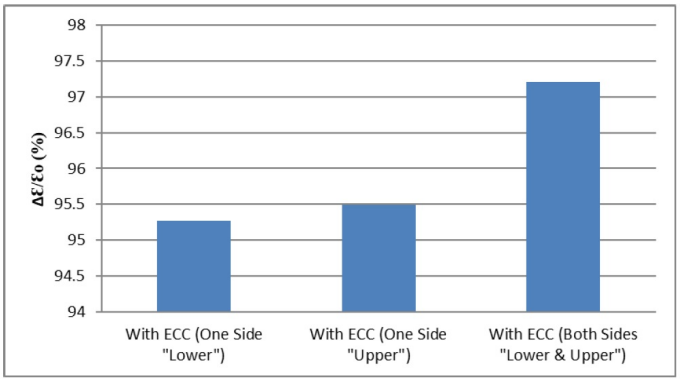

Figure 9: The effect of the ECC reinforcement layers and the location of these layers (with full connection) on the percentage of reduction in the plastic strain of the specimen of unreinforced masonry materials during vertical impact loading (t = 15 mm, E_{ecc}=17.5 GPa)

surface have a more significant performance in the uniform distribution of the plastic strains through the specimen, reducing the intensity of the plastic strains and cracks and failure of the specimen under impact loading.

The figures show the proper performance of the ECC reinforcement layers in uniform distribution of the plastic strains through the unreinforced masonry material specimen (reducing the intensity of plastic strains, cracks, and failure of the specimen) under impact loading and finally improving its out-plane dynamic impact behavior. With the two-sided cover of the specimen with ECC reinforcement layers (compared to the one-sided cover, especially on the lower surface of the specimen), this proper performance was more significant.

Fig. 10 also indicate the considerable reduction in the vertical impact displacement in the middle of the unreinforced

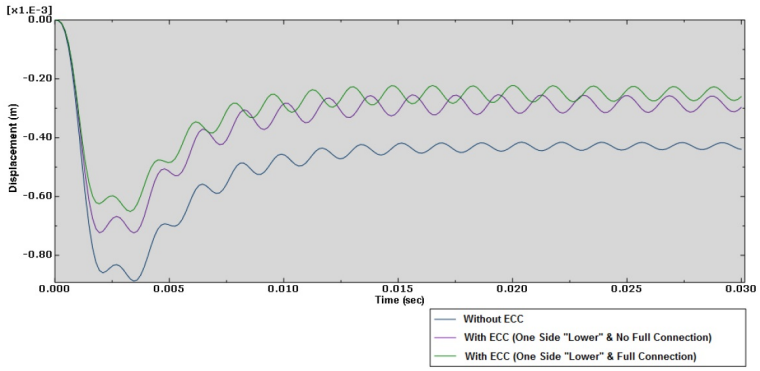

Figure 10: The effect of the ECC reinforcement layers and the location of these layers (with full connection) on the vertical displacement in the middle of the unreinforced masonry material specimen during vertical impact loading (t = 15 mm, E_{ecc}=17.5 GPa)

masonry material specimen due to the retrofitting with ECC layers (especially with full connection to the whole upper or lower surfaces of the specimen). Figures above indicate the proper performance of the ECC reinforcement layers in reducing the deflections of the unreinforced masonry material specimen under impact loading and finally improving its out-plane dynamic impact behavior. With the full connection of the ECC reinforcement layers to the upper or lower surfaces of the specimen (compared to the lack of full connection of ECC layers to these surfaces), this proper performance was more significant.

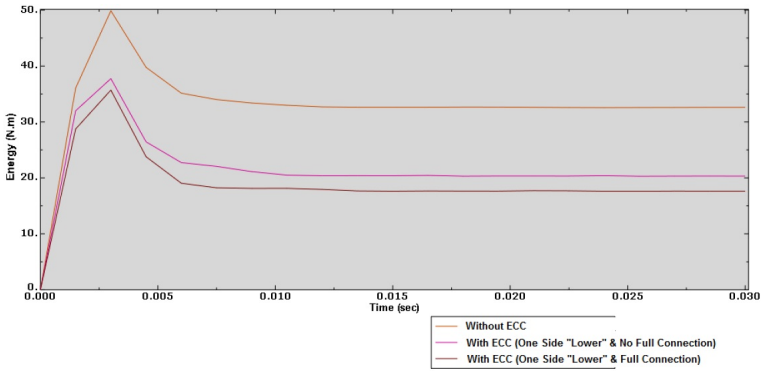

Figure 11: The effect of the ECC reinforcement layers and the connection type of these layers with the lower surface of the masonry materials on the energy of the unreinforced masonry material specimen during vertical impact loading (t = 15 mm, E_{ecc}=17.5 GPa)

Fig. 11 confirm the considerable energy dissipation (reduction) of the unreinforced masonry material specimen due to the retrofitting with ECC layers with the full connection to the whole upper or lower surfaces of the specimen under impact loading. The figures also show the proper performance of the ECC reinforcement layers in reducing the deflections of the unreinforced masonry material specimen under impact loading. Furthermore, it is finally improving its out-plane dynamic impact behavior. With the full connection of the ECC reinforcement layers to the upper or lower surfaces of the specimen (compared to the lack of full connection of ECC layers to these surfaces), this proper performance is more considerable.

Fig. 11 reveal the significant reduction in the concentration of the plastic strains in the edges of the unreinforced masonry material specimen retrofitted with ECC layers during impact loading. In addition, the figures show the uniform distribution of these stresses along the specimen (especially in areas of the ECC layers) and the remarkable reduction in the plastic strains, cracks, and failure of the specimen (especially with the full connection of ECC layers to the whole lower or upper surfaces of the specimen). The figures also confirm a good performance of the ECC reinforcement layers in the uniform distribution of plastic strains along the unreinforced masonry material specimen (reduction in the intensity of plastic strains, cracks, and failure of the specimen) under impact loading, resulting in improving its out-plane dynamic impact behavior. The full connection of the ECC reinforcement layers to the upper or lower surfaces of the specimen (compared to the lack of full connection of ECC layers to these surfaces) leads to an appropriate performance.

Figs. 12 and 13 represent that retrofitting the unreinforced masonry specimen with ECC layers (especially with a

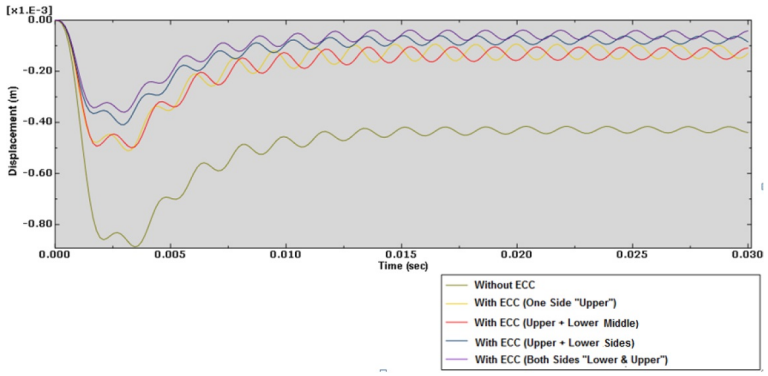

Figure 12: The effect of the ECC reinforcement layers and the location of the bottom layer (middle or edges of the bottom surface with full connection) in the two-sided cover on the vertical displacement in the middle of the unreinforced masonry material specimen during vertical impact loading (t = 15 mm, E_{ecc}=17.5 GPa)

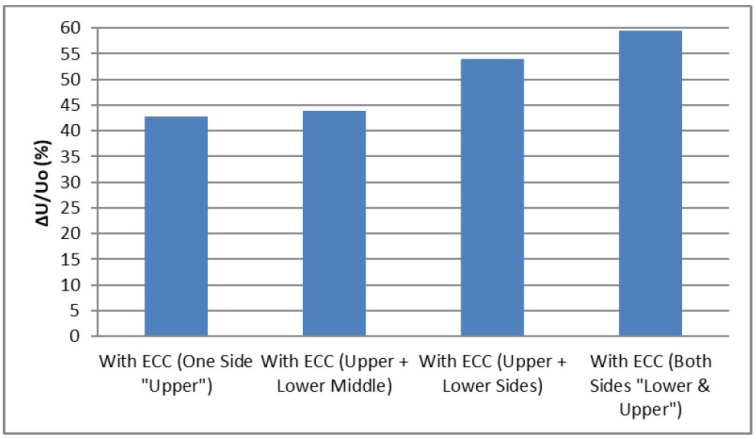

Figure 13: The location effect of the bottom layer (middle or edges of the bottom surface with full connection) in the two-sided cover on the percentage of reduction in the vertical displacement in the middle of the unreinforced masonry material specimen during vertical impact loading (t = 15 mm, E_{ecc}=17.5 GPa)

two-sided cover on the specimen's whole bottom and top surfaces) significantly reduces the vertical impact displacement in the middle of the specimen. It can also be shown that by retrofitting the unreinforced masonry material specimen with one ECC layer on the entire top surface and two ECC layers on the edges of the bottom surface of the specimen (compared to one ECC layer on the whole top surface of the specimen and one ECC layer in the middle of the bottom surface of the specimen), the ECC layers has a more significant performance (close to the performance of the two-sided cover on the whole top and bottom surfaces of the specimen) in increasing the out-plane strength and reducing the vertical displacement in the middle of the specimen during impact loading. By retrofitting the unreinforced masonry material specimen with one ECC layer on the entire top surface and one ECC layer in the middle of the bottom surface of the specimen, the ECC layers have a weaker performance (close to the performance of the one-sided cover on the whole top surface of the specimen) in the increment of the out-plane strength, and reduction of the vertical displacement in the middle of the specimen during impact loading.

The figures also indicate that the proper performance of the ECC reinforcement layers (especially on the whole top surface and edges of the bottom surface of the specimen) in the reduction of the deflections of the unreinforced masonry material specimen under impact loading improves its out-plane dynamic impact behavior. The two-sided cover of the specimen with ECC reinforcement layers (compared to the one-sided cover on the whole top surfaces of the specimen, cover in the whole top surface of the specimen and middle of the bottom surface of the specimen) leads to a significant performance.

Figs. 14 and 15 reveal that retrofitting the unreinforced masonry material specimen with ECC layers (especially with a two-sided cover on the whole bottom and top surfaces of the specimen) significantly reduced the energy dissipation (reduction) during impact loading. It can also be resulted that retrofitting the unreinforced masonry material specimen with one ECC layer on the entire top surface and two ECC layers on the edges of the bottom

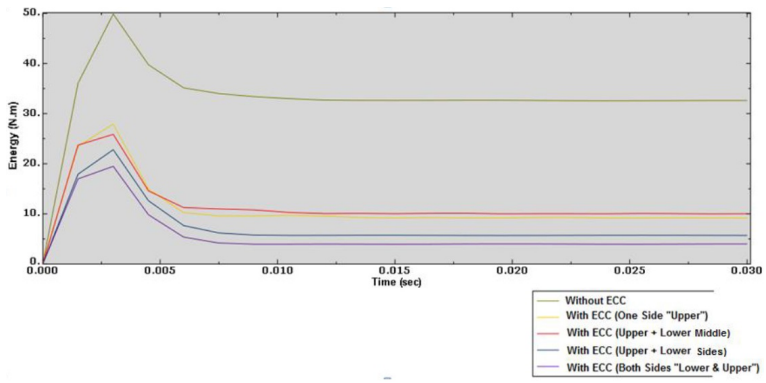

Figure 14: The effect of the ECC reinforcement layers and the location of the bottom layer (middle or edges of the bottom surface with full connection) in the two-sided cover on the energy of the unreinforced masonry material specimen during vertical impact loading (t = 15 mm, E_{ecc}=17.5 GPa)

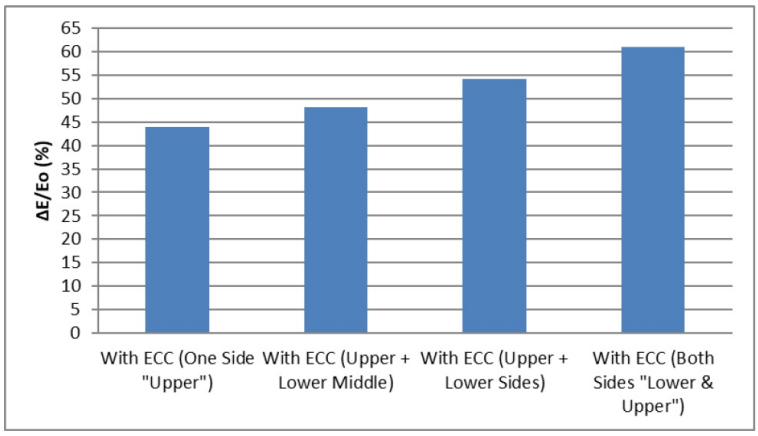

Figure 15: The location effect of the bottom layer (middle or edges of the bottom surface with full connection) in the two-sided cover on the percentage of reduction in the energy of the unreinforced masonry material specimen during vertical impact loading (t = 15 mm, E_{ecc}=17.5 GPa)

surface of the specimen leads that the ECC layers have a more significant performance (close to the performance of the two-sided cover on the whole top and bottom surfaces of the specimen) in absorbing the energy and, dissipating (reducing) the energy of the specimen during impact loading. In addition, retrofitting the unreinforced masonry material specimen with one ECC layer on the entire top surface and one ECC layer in the middle of the bottom surface of the specimen results that the ECC layers have a lower performance in absorbing energy during impact loading.

According to the figures, it can be found out that the ECC reinforcement layers (especially on the whole top surface and edges of the bottom surface of the specimen) significantly enhances the energy dissipating of the unreinforced masonry material specimen under impact loading and the out-plane dynamic impact behavior. With the two-sided cover of the specimen with ECC reinforcement layers (compared to the one-sided cover on the whole top surfaces of the specimen and cover in the whole top surface of the specimen and middle of the bottom surface of the specimen), this proper performance is more significant.

According to Fig. 16, retrofitting the unreinforced masonry material specimen with ECC layers (especially with a two-sided cover on the whole top and bottom surfaces of the specimen) remarkably decreases the concentration of the plastic strains in the edges of the specimen (and consequently cracking and failure of the specimen) under impact loading. The distribution of the concentrated strains and cracks (in the edges of the specimen) with a uniform trend through the specimen (especially in ECC layers) significantly reduces the intensity of plastic strains and cracks as well as failure of the unreinforced masonry material specimen retrofitted with ECC layers (especially with a two-sided cover on the whole top and bottom surfaces) during the impact loading. It can also be resulted that by retrofitting the unreinforced masonry material specimen with one ECC layer on the entire top surface and two ECC layers on the edges of the bottom surface of the specimen (compared to one ECC layer on the whole top surface of the specimen and one

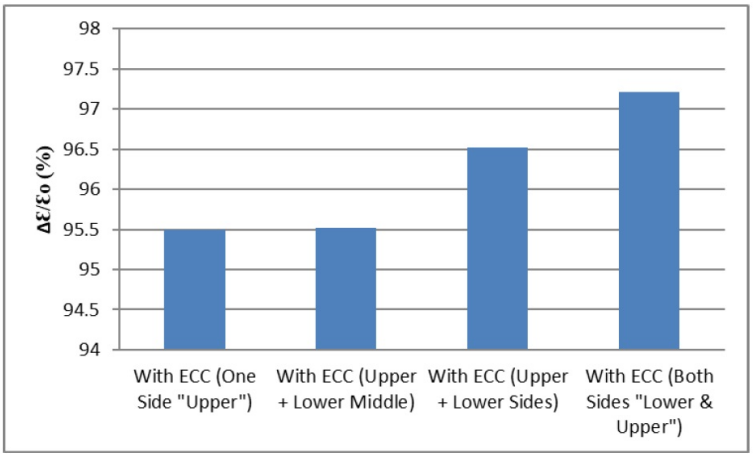

Figure 16: The location effect of the bottom layer (middle or edges of the bottom surface with full connection) in the two-sided cover on the percentage of reduction in the plastic strains of the unreinforced masonry materials during vertical impact loading (t = 15 mm, E_{ecc}=17.5 GPa)

ECC layer in the middle of the bottom surface of the specimen), the ECC layers has a more significant performance in the uniform distribution of plastic strains throughout the specimen, which eventually reduces the intensity of plastic strains, cracks and failure of the specimen during impact loading. By retrofitting the unreinforced masonry material specimen with one ECC layer on the entire top surface and one ECC layer in the middle of the bottom surface of the specimen, the ECC layers have a weaker performance (close to the performance of the one-sided cover on the whole top surface of the specimen) in the uniform distribution of plastic strains through the specimen, resulting in a reduction in the intensity of plastic strains, cracks and failure of the specimen during impact loading.

In general, the figures above show that the proper performance of the ECC reinforcement layers (especially on the whole top surface and edges of the bottom surface of the specimen) in the uniform distribution of plastic strains through the unreinforced masonry material specimen (reduced intensity of the plastic strains, cracks, and failure) under impact loading eenhances its out-plane dynamic impact behavior. The two-sided cover of the specimen with ECC reinforcement layers (compared to the one-sided cover on the whole top surfaces of the specimen, cover in the whole top surface of the specimen and middle of the bottom surface of the specimen) significantly rises the proper performance.

4 Conclusion

The strengthening of the unreinforced masonry specimen with ECC layers, specifically with double coverage on the top and bottom, significantly reduced the impact-induced vertical displacement in the middle of the unreinforced masonry specimen (particularly with double coverage and full ECC bonding across the bottom of the specimen). It also strongly enhanced energy absorption under the impact load, increasing energy dissipation (specifically with ECC layers fully bonded to the top or bottom surface of the specimen).

The specimen with an ECC layer across the bottom and an ECC layer on the sides of the top surface showed lower performance (similar to the specimen with an ECC layer across the top surface) in terms of out-of-plane strength enhancement and vertical displacement reduction in the middle under impact loading.

The strengthening of the unreinforced masonry specimen with ECC layers (specifically with double coverage) considerably reduced the plastic strain concentration on the sides of the specimen (and thus cracks and damage) under impact loading. The strains and cracks were distributed uniformly along the specimen (particularly in the ECC areas), substantially diminishing plastic strains, cracks, and damage within the ECC-strengthened unreinforced masonry specimen (particularly under full ECC bonding to the top or bottom surface).

The unreinforced masonry specimen strengthened with an ECC layer on the top surface and two ECC layers on the sides of the bottom surface showed higher performance than the specimen with the specimen strengthened with an ECC layer on top and an ECC layer in the middle of the bottom surface – and almost the same performance as the specimen with the one with double coverage throughout the top and bottom surfaces – in terms of out-of-plane strength enhancement and vertical displacement reduction in the middle under impact loading. The unreinforced masonry specimen with an ECC layer in the middle of the bottom surface showed lower performance (almost the

same as that of the specimen with a single-sided coverage across the top surface) in terms of out-of-plane strength enhancement and vertical displacement reduction in the middle under the impact load.

The unreinforced masonry specimen with two ECC layers on the sides of the bottom surface had a higher performance than the specimen with an ECC layer on the top surface and an ECC layer in the middle of the bottom surface and showed a similar performance to the specimen with double coverage across the top and bottom in terms of energy absorption and dissipation under impact loading. The specimen with an ECC layer in the middle of the bottom surface had a lower performance in energy absorption and dissipation under the impact load.

The unreinforced masonry specimen with an ECC layer across the bottom surface and two ECC layers in the middle of the top surface showed higher performance than the specimen with an ECC layer across the bottom surface and an ECC layer on each side of the top surface in terms of out-of-plane strength enhancement and vertical displacement reduction in the middle under the impact load. The specimen with an ECC layer across the bottom showed a lower performance in terms of out-of-plane strength enhancement and vertical displacement reduction in the middle under impact loading.

References

[1] K. Bergi, *Dynamics of Structures*, Tehran, Tehran University Publications, 2012.

[2] B. Borah, V. Singhal and H.B. Kaushik, *Sustainable housing using confined masonry buildings*, SN Appl. Sci. **1** (2019), no. 9, 1–7.

[3] G. Cai, Q. Su, K.D. Tsavdaridis and H. Degée, *Simplified density indexes of walls and tie-columns for confined masonry buildings in seismic zones*, J. Earthquake Eng. **24** (2020), no. 3, 447–469.

[4] M. Deng and S. Yang, *Cyclic testing of unreinforced masonry walls retrofitted with engineered cementitious composites*, Construct. Build. Mater. **177** (2018), 395–408.

[5] M. Deng and S. Yang, *Experimental and numerical evaluation of confined masonry walls retrofitted with engineered cementitious composites*, Engin. Struct. **207** (2020), 110249.

[6] D. Dizhur, J. Ingham, L. Moon, M. Griffith, A. Schultz, I. Senaldi, G. Magenes, J. Dickie, S. Lissel and J. Centeno, *Performance of masonry buildings and churches in the 22 February 2011 Christchurch earthquake*, Bull. New Zealand Soc. Earthquake Eng. **44** (2011), no. 4, 279–296.

[7] D.C. Drucker and W. Prager, *Soil mechanics and plastic analysis or limit design*, Quart. Appl. Math. **10** (1952), no. 2, 157–165.

[8] M. Endait and S. Kolhe, *Experimental investigation of engineered cementitious composites (ECC) retrofitted masonry structures*, SN Appl. Sci. **2** (2020), no. 3, 1–11.

[9] D.C. Kent and R. Park, *Flexural members with confined concrete*, J. Struct. Div. **97** (1971), no. 7, 1969–1990.

[10] Y.Y. Kim, H.-J. Kong and V.C. Li, *Design of engineered cementitious composite suitable for wet-mixture shotcreting*, Mater. J. **100** (2003), no. 6, 511–518.

[11] M. Li and V.C. Li, *Behavior of ECC/concrete layer repair system under drying shrinkage conditions*, Restorat. Build. Monum. **12** (2006), no. 2, 143–160.

[12] V.C. Li, D.K. Mishra, A.E. Naaman, J.K. Wight, J.M. LaFave, H.-C. Wu and Y. Inada, *On the shear behavior of engineered cementitious composites*, Adv. Cement Based Mater. **1** (1994), no. 3, 142–149.

[13] Y.-W. Lin, L. Wotherspoon, A. Scott and J.M. Ingham, *In-plane strengthening of clay brick unreinforced masonry wallets using ECC shotcrete*, Engin. Struct. **66** (2014), 57–65.

[14] J. Lubliner, J. Oliver, S. Oller and E. Oñate, *A plastic-damage model for concrete*, Int. J. Solids Struct. **25** (1989), no. 3, 299–326.

[15] N. Lundgren, M. Ekevad and J. Flodin, *ABAQUS analysis users' manual ABAQUS analysis users' manual, 2007*, J. Wood Sci. **57** (2011), no. 2, 94–99.

[16] M. Maalej, V. Lin, M. Nguyen and S. Quek, *Engineered cementitious composites for effective strengthening of unreinforced masonry walls*, Engin. Struct. **32** (2010), no. 8, 2432–2439.

[17] M. Maalej, S.T. Quek and J. Zhang, *Behavior of hybrid-fiber engineered cementitious composites subjected to dynamic tensile loading and projectile impact*, J. Mater. Civil Engin. **17** (2005), no. 2, 143–152.

[18] G. Magenes and G.M. Calvi, *In-plane seismic response of brick masonry walls*, Earthquake Engin.Struct. Dyn. **26** (1997), no. 11, 1091–1112.

[19] M. Najafgholipour, S. Dehghan and A. Kamrava, *In-plane shear behavior of masonry walls strengthened with steel fiber-reinforced concrete overlay*, Asian J. Civil Eng. **19** (2018), no. 5, 553–570.

[20] A.N. Niasar, F.J. Alaee and S.M. Zamani, *Experimental investigation on the performance of unreinforced masonry wall, retrofitted using engineered cementitious composites*, Construct. Build. Mater. **239** (2020), 117788.

[21] C.G. Papanicolaou, T.C. Triantafillou, K. Karlos and M. Papathanasiou, *Textile-reinforced mortar (TRM) versus FRP as strengthening material of URM walls: In-plane cyclic loading*, Mater. Struct. **40** (2007), no. 10, 1081–1097.

[22] C. Papanicolaou, T. Triantafillou and M. Lekka, *Externally bonded grids as strengthening and seismic retrofitting materials of masonry panels*, Construct. Build. Mater. **25** (2011), no. 2, 504–514.

[23] S.-H. Park, N.H. Dinh, S.-H. Kim, J.-W. Hwang, H.H. Pham, S.-J. Lee and K.-K. Choi, *Seismic retrofit of unreinforced masonry walls using precast panels of fiber-reinforced cementitious composite*, J. Build. Eng. **53** (2022), 104548.

[24] R. Park and T. Paulay, *Reinforced Concrete Structures*, John Wiley & Sons, 1975.

[25] S. Pourfalah, D.M. Cotsovos and B. Suryanto, *Modelling the out-of-plane behaviour of masonry walls retrofitted with engineered cementitious composites*, Comput. Struct. **201** (2018), 58–79.

[26] S. Pourfalah, B. Suryanto and D.M. Cotsovos, *Enhancing the out-of-plane performance of masonry walls using engineered cementitious composite*, Composit. Part B: Engin. **140** (2018), 108–122.

[27] S. Renuka and I. Mervin Sanjith, *Strengthening of damaged masonry walls using engineered cementitious composites: Experimental and numerical analysis*, Adv. Civil Eng. **2022** (2022).

[28] M. Rezaei, A. Hamidi and A. Farshi Homayoun Rooz, *Investigation of peak particle velocity variations during impact pile driving process*, Civil Engin. Infrastruct. J. **49** (2016), no. 1, 59–69.

[29] Z. Riahi, K.J. Elwood and S.M. Alcocer, *Backbone model for confined masonry walls for performance-based seismic design*, J. Struct. Eng. **135** (2009), no. 6, 644–654.

[30] S. Singh, R. Patil and P. Munjal, *Study of flexural response of engineered cementitious composite faced masonry structures*, Engin. Struct. **150** (2017), 786–802.

[31] M. Shokri and A. Darviza, *Guilan*, Publications of University of Guilan, 2012.

[32] A. Tabrizikahou, M. Kuczma, M. Łasecka-Plura and E. Noroozinejad Farsangi, *Cyclic behavior of masonry shear walls retrofitted with engineered cementitious composite and pseudoelastic shape memory alloy*, Sensors **22** (2022), no. 2, 511.

[33] B. Tahmouresi, P. Nemati, M.A. Asadi, A. Saradar, and M.M. Moein, *Mechanical strength and microstructure of engineered cementitious composites: A new configuration for direct tensile strength, experimental and numerical analysis*, Construct. Build. Mater. **269** (2021), 121361.

[34] M. Tomaževič and I. Klemenc, *Verification of seismic resistance of confined masonry buildings*, Earthquake Engin. Struct. Dyn. **26** (1997), no. 10, 1073–1088.

[35] G.P. Van Zijl, *Improved mechanical performance: Shear behaviour of strain-hardening cement-based composites (SHCC)*, Cement Concrete Res. **37** (2007), no. 8, 1241–1247.

[36] J. Zhang, M. Maalej and S. Quek, *Hybrid fiber engineered cementitious composites (ECC) for impact and blast-resistant structures*, Proc. First Int. Conf. Innov. Mater. Technol. Construct. Restor.–IMTCR04, 2004, pp. 136–149.